Proceedings of the ASME 2019
International Mechanical Engineering Congress and Exposition
IMECE2019
November 11-14, 2019, Salt Lake City, UT, USA

IMECE2019-10122

EXPERIMENTAL STUDY OF PARTIAL FUEL SUBSTITUTION WITH HYDROXY AND ENERGY RECOVERY IN LOW DISPLACEMENT COMPRESSION IGNITION ENGINES

Jorge Duarte Forero[1] *, Natalia Duarte[1], Brando Hernandez[1], Marley Vanegas[2]
[1]Universidad del Atlántico
Department of Mechanical Engineering
Barranquilla, Colombia
[2]Universidad del Atlántico
Department of Chemical Engineering
Barranquilla, Colombia

Ricardo Stand[3]
[3]Sphere Energy
Barranquilla, Colombia

ABSTRACT

Internal combustion engines only take advantage of a quantity of the energy available in the combustion process. In addition to this, the emissions generated alter the balance and natural composition of the air, which represents a current risk to human health. Because of this, to reduce the dependence on fossil fuels and minimize the harmful emissions to the environment of this type of thermal machines, in this work, the implementation of an exhaust gas energy recovery system is proposed. With the recovered energy, is hydroxy through the electrolysis process, and so that partial substitution of diesel fuel with the gaseous fuel produced. For the experimental study, a diesel engine SOKAN SK-MDF300 is coupled to a thermoelectric generator formed by Peltier modules, which transform thermal energy into electrical energy. This energy was used to generate hydroxy, reaching a generation maximum of 1.37 L / min. The influence of the partial substitution using diesel fuel and B10 fuel was studied. The experimental results allow us to conclude that a 3% reduction in fuel was achieved with diesel fuel. In addition to this, CO_2 emissions were reduced in 13%, CO in 11.66%, NOx in 35.38%, SOx in 14.84% and 21.69% of reduction in smoke opacity, in the condition of maximum load during the test in the engine. The implementation of the TEG, coupled with the HHO gas generation system increases the overall efficiency of the engine by 4.2%.

Keywords: Biodiesel, diesel, emission, hydroxy, thermoelectric generator.

NOMENCLATURE

$\dot{W}$	Power [$\dot{W}$]
$\dot{m}$	Mass flow rate [kg/s]
CV	Calorific value [MJ/kg]
η	Efficiency
HSU	Hartridge smoke unit
ppm	Parts per million
%	Percentages of volume
rpm	Revolution per minute
HEX	Heat exchanger
TEM	Thermoelectric modules
TEG	Thermoelectric generator
NOx	Nitrogen oxides
SOx	Sulfur oxides
CO	Carbon monoxide
CO_2	Carbon dioxide
KOH	Potassium Hydroxide

1. INTRODUCTION.

At present, the demand for fossil fuels has increased, which has generated concern in the world for its limited availability and high levels of pollutants in the atmosphere, causing severe problems such as global warming [1]. Therefore, in the last decades, different investigations have been developed in search of reductions in fuel consumption and emissions of internal

[1] Contact author: jorgeduarte@mail.uniatlantico.edu.co

combustion engines (ICE), without requiring drastic changes in the design of the engine [2, 3]. Among these investigations is the use of alternative fuels such as H_2 [4, 5].

Hydrogen is recognized as a non-polluting, renewable, and recyclable fuel. It has different advantages such as its wide flammability range, low ignition energy, small extinguishing distance, high autoignition temperature, high flame speed in stoichiometric ratios, high diffusivity and very low density [6]. It has been shown that the use of hydrogen gas as a fuel in ICEs has produced higher power in the engine and lower concentrations of pollutants in the exhaust gases [7, 8]. Ma et al. [9] showed that the mixture of H_2 and natural gas produces shorter periods of development and propagation of the flame so that the efficiency of the combustion increases and the emission levels are lower. On the other hand, the addition of HHO in the ICE was studied by Yilmaz et al. [10] their results show an increase in the engine torque in an average of 19.1%, a reduction in the emissions of CO and hydrocarbons (HC) and the specific fuel consumption (SFC) in averages of 13.5%, 5%, and 14%, respectively.

The study by Ji and Wang [11] showed the effect of the addition of hydrogen on engine performance. The results indicated that the use of hydrogen improved the thermal efficiency of the brakes by 26.37-31.56%, with a hydrogen mixing level of 6%. Also, HC and CO_2 emissions are reduced, but NOx emissions increase with increasing hydrogen addition.

The most researched method for the implementation of hydrogen in ICE is through the use of hydrogen cells, especially for its efficiency in partial loads, its silent operation, and its modularity [12]. Engines with hydrogen cells partially replace the fuel with hydrogen, which is stored in tanks that are occasionally filled [13]. Musmar and Al-Rousan [7] tested a compact HHO generation device on a gasoline engine. Their results showed that nitrogen oxides (NOx), carbon monoxide (CO) and fuel consumption were reduced by 50%, 20%, and 30%, respectively. An HHO fuel production unit based on the electrolysis process was designed and built with the ability to alter the distances between the anode-cathode plates, which was integrated into a Honda G 200 (197 cc single-cylinder engine). Hydrocarbon (HC) and carbon monoxide emissions were reduced to approximately 40% at different operating speeds. It was considered that the 5 mm gap has the most significant impact on reducing emissions [14].

The main drawback of the use of hydrogen cells is their need for a source of energy to start the electrolysis process that will form hydrogen. In search of alternatives that do not affect the efficiency of the engine, the present study investigates the implementation of a thermoelectric generator (TEG) installed in the engine exhaust system [15]. The TEG is composed of thermoelectric modules (TEMs), which directly convert thermal energy into electrical energy, which is used to power a hydroxy generating device. The intake manifold for the hydroxy gas injection was modified near the intake ports, to study the effect on the HHO gas addition in the performance and the emissions of CO, CO_2, HC, and NOx, to different rpm and torque of the engine.

2. MATERIALS AND METHODS

2.1 Thermoelectric generator (TEG)

Thermoelectric generators are solid-state energy harvesters that can directly convert thermal energy into electrical energy from a temperature difference. The TEG used in this study is composed of a heat exchanger, thermoelectric modules, and cooling system. Figure 1 shows the thermoelectric generator used and the description of the thermoelectric modules.

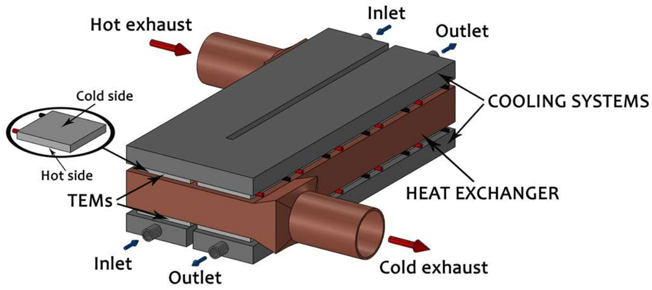

(a)

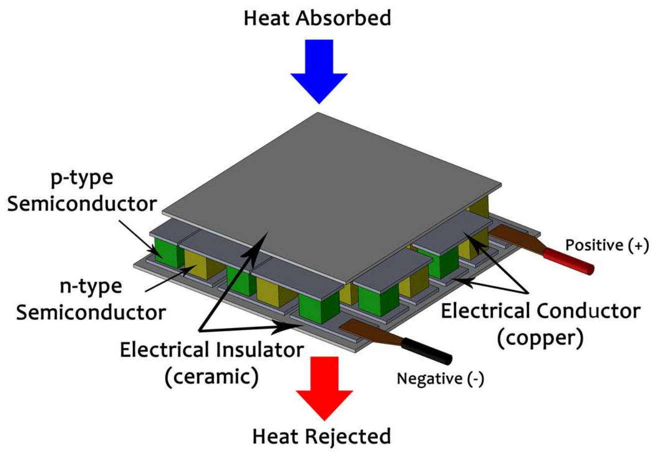

(b)

FIGURE 1. (a) Thermoelectric generator (TEG), (b) thermoelectric modules (TEMs).

2.1.1. Heat exchanger (HEX) and thermoelectric modules (TEMs)

Figure 2 shows the heat exchanger used. The HEX is of the rectangular internal conduit type with dimensions of 95 mm x 227 mm x 24 mm. Its interior is composed of a series of deflectors (see Fig. 2b) that allow increasing the residence time of the exhaust gases, which increases the amount of heat transferred from the exhaust gases to the outer walls of the HEX.

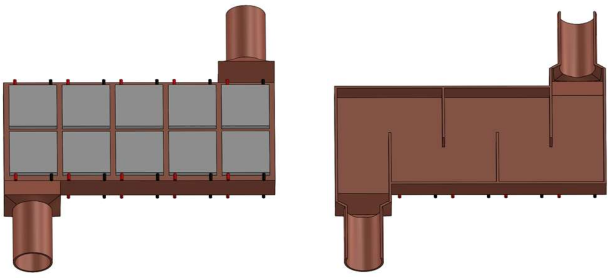

FIGURE 2. (a) Structure of the hex that shows the matrix of the TEMs, (b) sectioned view that shows the internal geometry of the hex.

A total of 20 thermoelectric modules were placed on the external surface of the heat exchanger (ten on its upper surface and ten on the lower surface) with an array of 5 x 2 (see Fig. 2a). A thin layer of thermal paste was applied between the external surface of the heat exchanger and the thermoelectric modules, to increase the heat conduction. The thermoelectric modules used in this study are model TEG1-12610-5.1, which can operate at a maximum temperature of 300 °C on the hot side.

2.1.2. Cooling system

To maintain a temperature difference in each thermoelectric module, two rectangular coolers with dimensions of 95 x 227 x 12 mm, are placed above the TEMs. The thermal paste is applied between the coolers and TEMs, to increase the heat conduction, and compensate the mechanical tolerances and the height differences between the TEMs.

For each of the rectangular coolers, the coolant (i.e., water) is circulated using a pump. The refrigerant loses heat when it passes through a chiller with a capacity of 30 liters.

2.2. HHO gas generation system

2.2.1. Electrolysis process

The electrolysis of water is the process of decomposition of water into hydrogen and oxygen with the passage of electric current through water.

To carry out this process, a hydrogen cell formed by electrodes and electrolyte, linked to a source of electrical energy, can be used. The power source is connected to two electrodes (anode and cathode). During electrolysis, hydrogen will be generated at the cathode, and oxygen will be produced at the anode; the amount of hydrogen generated will be double that of oxygen. The reaction that takes place in the electrodes, and the general reaction is the following [16]:

Cathode (reduction):

$$2H_2O_{(l)} + 2e^- \rightarrow H_{2(g)} + 2OH^-_{(aq)} \quad (1)$$

Anode (oxidation):

$$4OH^-_{(aq)} \rightarrow O_{2(g)} + 2H_2O_{(l)} + 4e^- \quad (2)$$

Global reaction:

$$2H_2O_{(l)} \rightarrow 2H_{2(g)} + O_{2(g)} \quad (3)$$

The process of obtaining HHO gas is a bit more complicated than electrolysis, although it follows the same principle, two electrodes submerged in water. In the process, the water separates into its diatonic molecules and slightly recombines again, giving rise to the HHO gas [17].

2.2.2. System description

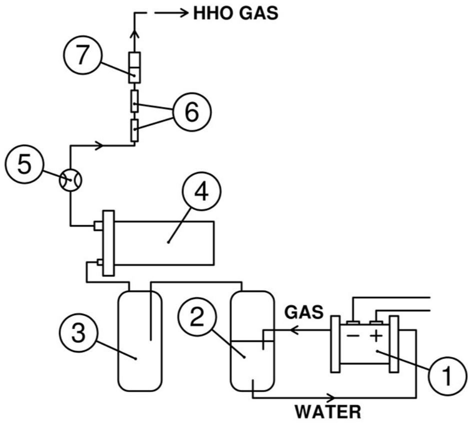

FIGURE 3. Schematic diagram of the HHO gas generation system.

The HHO gas generator system used in this study is shown in Figure 3. It consists of a dry cell (1), an electrolytic tank (2), a bubbler (3), an HHO gas storage tank (4) and an HHO gas flow meter (5). As security measures were installed flame arrester (6) and silica gel filter (7) in the line.

2.2.3. Dry cell

Stainless steel was used for the electrodes in the dry cell, as it is highly corrosion resistant, non-reactive with the electrolyte, good conductor and capable of withstanding high temperature and voltage. 7 electrodes with dimensions of 13.3 x 20.3 x 0.1 cm were used. The space between the adjacent electrodes was limited to 0.2 cm with neoprene gaskets. Also, acrylic plates with dimensions of 16.1 x 23.3 x 1.0 mm were used to provide a visual indication of the electrolyte level. The dry cell is fed with the electrical energy recovered from the TEG.

To increase the productivity of the cell, a catalyst was used. According to studies, NaOH, KOH, and NaCl can be used for the production of HHO gas. However, KOH has been widely used in electrolyzers due to its high conductivity [18]. In this study, the KOH catalyst is used at a concentration of 20% mass of solute in grams/volume of solution in mL.

2.3. Experimental facilities

A data acquisition system is used to measure and store the experimental data of the TEG. The system includes a temperature measurement circuit and a circuit to measure the currents and voltages of the TEMs.

The thermoelectric generator device is coupled to a diesel engine test bench (see Fig. 4). The engine specifications are shown in Table 1 [19].

Engine type	**Single - cylinder**
Manufacturer	SOKAN
Model	SK-MDF300
Cycle	4 - Stroke
Bore x stroke	78 mm x 62.57 mm
Displaced volume	299 CC
Compression ratio	20:1
Maximum power	4.6 hp to 3600 rpm
Intake system	Naturally aspirated
Injection system	Direct injection
Injection Angle	20° BTDC

TABLE 1. Specifications of the test engine

Figure 4 shows the schematic diagram of the configuration used in the experiments. The diagram consists of two coupled test benches, the Diesel engine test bench, and the TEG test bench, which is connected to the HHO gas generation system.

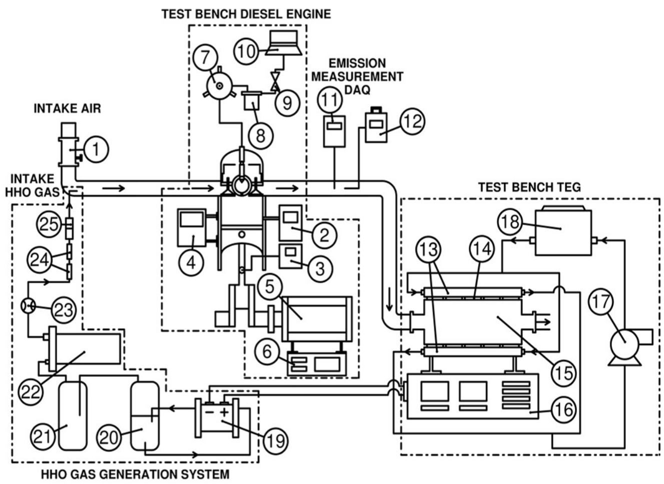

TEST BENCH DIESEL ENGINE: 1. Air Flowmeter, 2. In-cylinder pressure DAQ, 3. Encoder, 4. Median variables DAQ, 5. Alternator, 6. Resistive test bench, 7. Injection pump, 8. Fuel filter, 9. Fuel inlet valve, 10. Gravimetric fuel meter. **EMISSION MEASUREMENT DAQ:** 11. Exhaust gas analyzer, 12. Opacimeter. **TEST BENCH TEG:** 13. Cooling exchanger, 14. Thermoelectric module, 15. Heat exchanger, 16. Thermoelectric generator DAQ, 17. Water pump, 18. Chiller. **HHO GAS GENERATION SYSTEM:** 19. Dry cell, 20. Electrolytic tank, 21. Bubbler, 22. Storage tank HHO gas, 23. HHO Flowmeter, 24. Flame arrester, 25. Silica gel filter.

FIGURE 4. Schematic diagram of the experimental test bench.

Figure 5 shows the experimental test bench used in the study.

FIGURE 5. Experimental test bench

The experimental bench is formed by an engine test bench (1), the TEG test bench (2) and the HHO gas generation system (3).

2.4. Exhaust gas analyzer

A gas analyzer BrainBee AGS-688 (electromagnetic class E2), was used, applying the international recommendation OIML R 99-1 & 2, which defines the instruments to measure the exhaust emissions, the technical requirements, and the control of metrological and performance tests. In addition to this, the opacity of the exhaust gases is monitored using an opacimeter BrainBee OPA-100. Table 2 shows the details of the gas analyzers.

Equipment name	Model	Measuring element	Upper limit	Resolution
Brain Bee	AGS-688	CO	9.99 vol%	0.01
		CO_2	19.9 vol%	0.1
		NOx	5000 ppm	1
Brain Bee	OPA-100	Opacity	99.9 %	0.1

Table 2. Characteristics of the gas analyzers.

The uncertainty was calculated by analyzing the accuracy and precision of the instruments, together with the repeatability of the measurement. Three measurements were taken from each experiment. The average values are used for graphic representation.

2.5. Experimental Procedures

For the experimental process, four (4) modes of engine operation were tested. The selection of each operating mode is implemented by controlling a dynamometric brake. The sequence of selection of the operating modes consists of changes in the speed of the engine, maintaining a constant torque and changes in the torque, maintaining a constant speed of the engine. In this way, the effects due to the change in speed and torque can be analyzed independently. Torque and engine rpm was measured by sensors and processed by data logging from the engine test bench. The variation in the load of the engine is controlled through a resistive test bench connected to the electric alternator, which is coupled to the engine and allows to determine the amount of electrical energy generated.

The operating modes were selected to cover the largest area below the characteristic curve of the engine, in such a way that a large operating range of the engine is represented, and similarity is established with the emission cycle analyzes. Figure 6 shows the operation modes used in the experimental process.

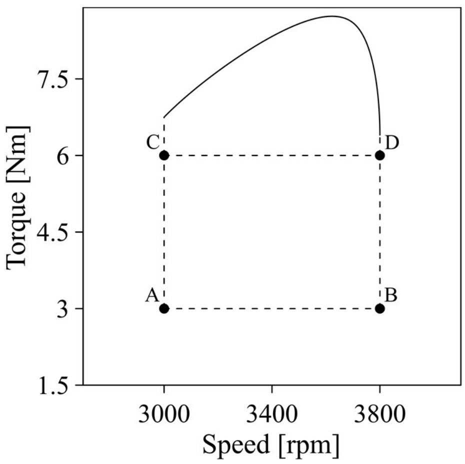

FIGURE 6. Modes of engine operation used for the experimental study.

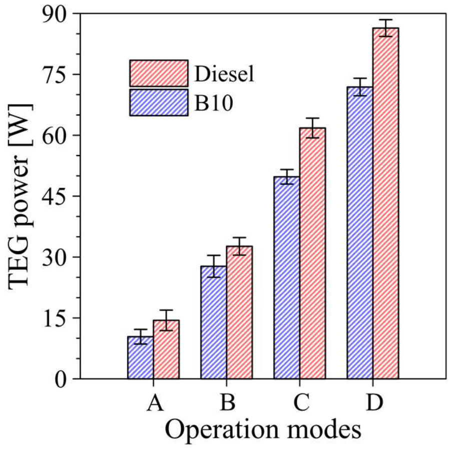

FIGURE 7. Power generated by the TEG for different operation modes.

Also, two types of fuels, Diesel and Biodiesel of 10% (B10) were used for each mode of operation. Table 3 shows the physicochemical properties of fuels.

Property	Units	Standards	Diesel	B10
Density	[kg/m^3]	ASTM D1298	821.5	827.5
Viscosity	[cSt]	ASTM D445	2.64	2.66
Flash point	[°C]	ASTM D93	76	96
Cloud point	[°C]	ASTM D2500	6.5	8.3
Pour point	[°C]	ASTM D97	3.1	3.8
Calorific value	[MJ/kg]	ASTM D240	44.05	43.25

TABLE 3. Physicochemical properties of fuels.

3. RESULTS AND DISCUSSION

3.1. Power output TEG

Figure 7 shows the power generated by the TEG for each of the modes of operation of the engine for the different fuels.

It is observed that the use of diesel fuel produces a higher recovery power compared to B10. This effect is more marked by increasing the rpm and the engine torque. In the operating mode D, the maximum power generated by the TEG is obtained, which is 72 W and 86 W, for the B10 and Diesel, respectively.

3.2. Recovery percentage

To measure the efficiency of the TEG, the percentage of energy recovery is calculated. This percentage is calculated with the following equation:

$$\eta_{ER} = \frac{\dot{W}_{TEG}}{\dot{W}_{eng}} \quad (4)$$

Where $\dot{W}_{TEG}$ and $\dot{W}_{eng}$ are the electrical output power of the TEG and the electrical power of the engine in its operating modes. Figure 8 shows the comparison of the recovery percentage for each fuel.

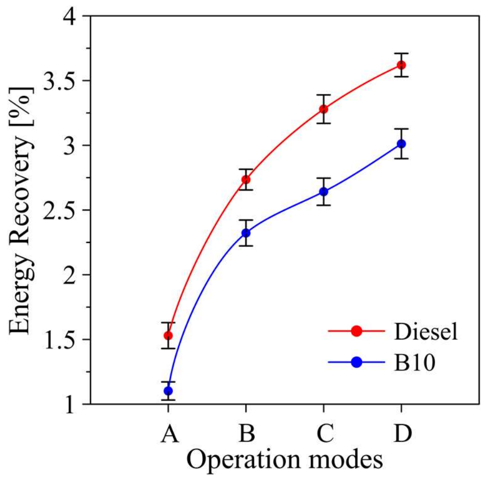

FIGURE 8. Energy recovery for different operation modes.

It is observed that the energy recovery increases with the rpm and the engine torque. Because the increase of these parameters produces an increase in the temperature of the exhaust gases, which allows obtaining a greater power in the TEMs. The maximum percentage of energy recovery was obtained with Diesel in operation mode, and its value is 3.62%.

3.3. HHO gas generation

Figure 9 shows the effect of the fuel in the generation of HHO gas.

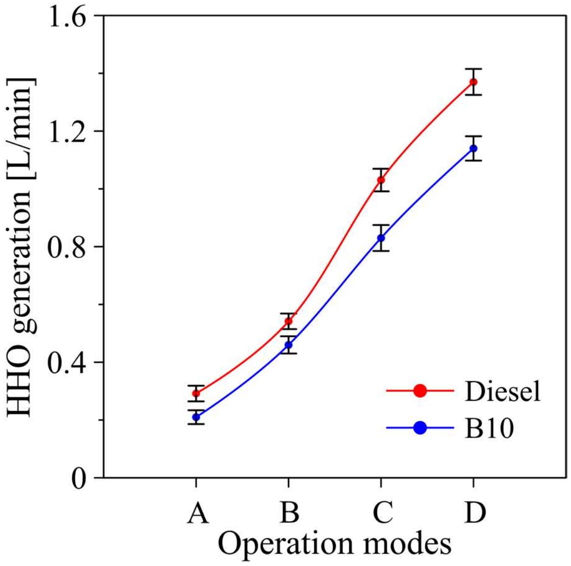

.

FIGURE 9. Generation of HHO gas for different operation modes.

It is observed that, on average, Diesel generates 22% of HHO gas when compared to B10. The rpm and torque increase of the engine allows increasing the generation of the HHO gas.

3.4. Global efficiency

Since the TEG generates additional power and the generation of HHO gas reduces fuel consumption, the implementation of both influences the global efficiency of the ICE. The global efficiency was defined with the following equation:

$$\eta_G = \frac{\dot{W}_{E,eng} + \dot{W}_{E,TEG}}{\dot{m}_{fuel} CV} \quad (5)$$

where $\dot{W}_{E,eng}$, $\dot{W}_{E,TEG}$, $\dot{m}_{fuel}$ and CV is the electrical power of the engine, the electrical power recovered by the TEG, the mass flow of fuel and the calorific value of the fuel, respectively.

Figure 10 shows the comparison of the overall efficiency of ICE using Diesel and B10 with HH0 gas. It is observed that, on average, the addition of HHO gas added to the use of TEG produces an increase in global efficiency of 4.16% y 3.81% with Diesel and B10, respectively.

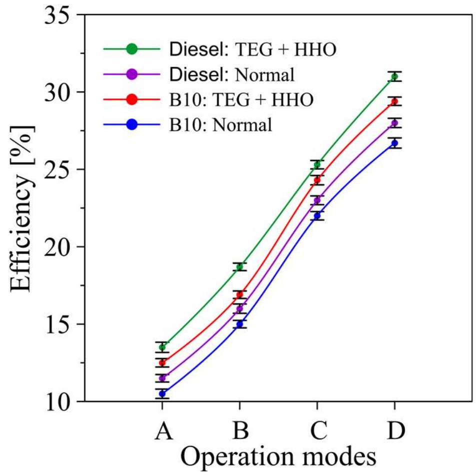

FIGURE 10. Global Efficiency of ICE with (a) Diesel, (b) B10.

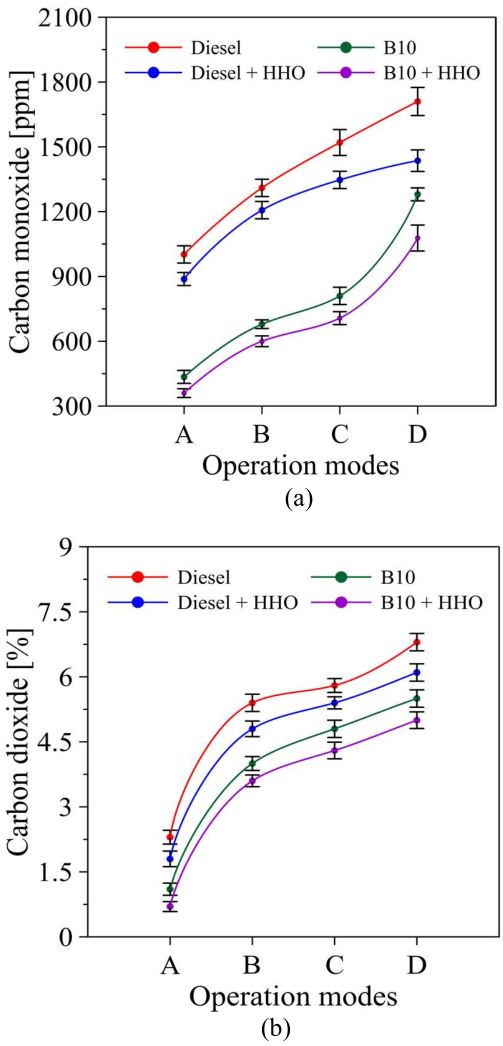

FIGURE 11. (a) CO and (b) CO_2, emissions for fuels tested.

3.5. Engine emissions

Figure 11 shows the effect of supplying HHO gas in the engine on CO and CO_2 emissions. It was observed that the HHO gas caused a reduction of 11.66% and 13%, in the CO emissions using Diesel and B10, respectively. Because CO depends to a large extent on the fuel/air ratio, the use of HHO gas significantly reduces the presence of CO by reducing fuel consumption.

The decrease in fuel consumption also results in a higher percentage of excess air in the exhaust, which reduces the presence of CO_2. It was observed that the addition of HHO decreases CO_2 emissions by 12.5% and 16.46%, using Diesel and B10, respectively.

Figure 12 shows the effect of supplying HHO gas in the engine on the NOx and SOx emissions. It was observed that the HHO caused an average reduction of 35.38% and 13.56%, in NOx emissions using Diesel and B10, respectively. NOx emissions are related to high temperatures in combustion. The introduction of HHO gas in the intake manifold reduces the amount of fuel, causing a reduction in the combustion temperature. Therefore, lower NOx emission is obtained. Concerning SOx emissions, a reduction of 14.84% and 20.87% was observed with Diesel and B10, respectively.

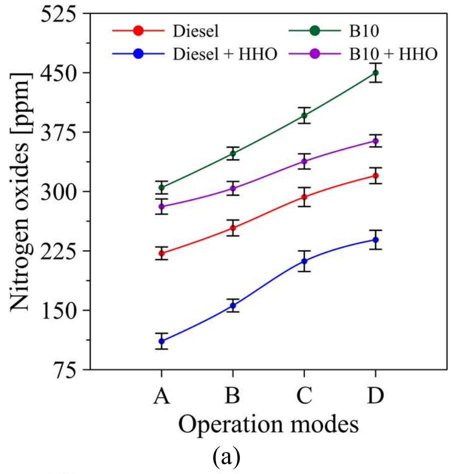

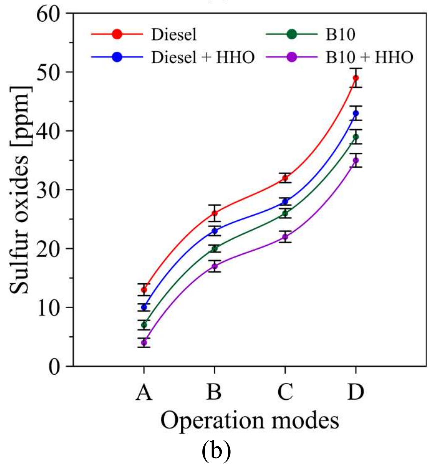

FIGURE 12. (a) NOx and (b) SOx, emissions for fuels tested.

Figure 13 compares the amount of smoke emitted by the test engine during its combustion without and with HHO gas. When HHO gas is added in the combustion process, the smoke is substantially reduced. This is attributed to the fact that the presence of HHO gas in the combustion process contributes to the formation of homogeneous mixtures, which reduces the smoke. A reduction of 21.69% and 22.63% was observed in Diesel and B10.

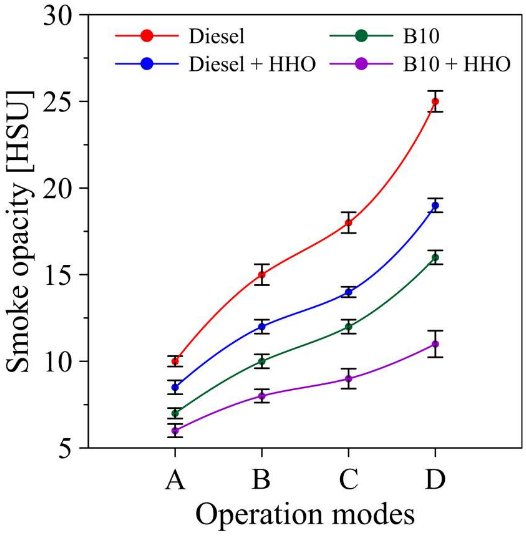

FIGURE 13. Smoke opacity for fuels tested.

The uncertainty on the values presented in Figures 11, 12 and 13 is due to the variability of the engine operation, to hidden variables that were not considered in the experiment and to the measurement error of the instruments.

4. CONCLUSION

The most important conclusions that can be inferred in this paper are the following:

The HHO gas generation system is easily incorporated with the engine intake system. The design of the system considers the safety requirements necessary for the addition of HHO gas in the combustion chamber. Concerning the installation of the TEG, it was found that the internal geometry of the heat exchanger produces a low-pressure drop. Therefore, there are no effects of backpressures in the exhaust system of the engine.

The implementation of the TEG allows generating a 71.88 W and 86.39 W with the fuel B10 and Diesel, in the conditions of the maximum load of the engine, which represents 3% and 3.62% of the engine's working power. This behavior is attributed to the higher calorific value present in diesel, which allows higher temperatures to be obtained on the external surface of the heat exchanger, causing a greater temperature difference in the TEMs.

The KOH catalyst with a concentration of 20%, allows a maximum generation of 1.37 L / min and 1.14 L / min, with Diesel fuel and B10, respectively.

The decrease in fuel consumption produced by the HHO gas generator and the power generated by the TEG increase the global efficiency of the system by 4.16%.

The B10 has a lower amount of CO, CO_2, SOx, and smoke emissions, compared to Diesel. However, NOx emissions were higher in B10. On average B10 fuel produces 37% more NOx when compared to Diesel.

In general, the concentrations of the emissions were reduced with the addition of HHO gas in the combustion chamber. On average, there was a maximum reduction of 15.89%, 9.64%, 22.15%, 11.14%, and 22.16% in the emissions of CO, CO_2, NOx, SOx, and smoke opacity.

Acknowledgments

The authors thank the UNIVERSIDAD DEL ATLÁNTICO and the SPHERE ENERGY company for their support on the development of this research.

J. Duarte Forero thank the support provided by Colombian Institute for Scientific and Technological Development (COLCIENCIAS) through the "Convocatoria Nacional para Estudios de Doctorado en Colombia año 2012".

REFERENCES

[1] A. Keskin, A. Yaşar, M. Gürü, and D. Altıparmak. Usage of methyl ester of tall oil fatty acids and resinic acids as alternative diesel fuel. *Energy Conversion and Management*, 51(12): 2863-2868, 2010.

[2] J. E et al. Effect of different technologies on combustion and emissions of the diesel engine fueled with biodiesel: A review. *Renewable and Sustainable Energy Reviews*, 80: 620-647, 2017.

[3] B. Mohan, W. Yang, and S. Chou. Fuel injection strategies for performance improvement and emissions reduction in compression ignition engines—A review. *Renewable and Sustainable Energy Reviews*, 28: 664-676, 2013.

[4] N. Usta et al. Combustion of biodiesel fuel produced from hazelnut soapstock/waste sunflower oil mixture in a Diesel engine. *Energy Conversion and Management*. 46(5): 741-755, 2005.

[5] M. Sadiq Al-Baghdadi and H. Shahad Al-Janabi. Improvement of performance and reduction of pollutant emission of a four-stroke spark-ignition engine fueled with hydrogen–gasoline fuel mixture. *Energy Conversion and Management*, 41(1): 77-91, 2000.

[6] T. Su, C. Ji, S. Wang, L. Shi, J. Yang, and X. Cong. Investigation on performance of a hydrogen-gasoline rotary engine at part load and lean conditions. *Applied Energy*, 205: 683-691, 2017.

[7] A. Al-Rousan. Reduction of fuel consumption in gasoline engines by introducing HHO gas into intake manifold. *International Journal of Hydrogen Energy*. 35(23): 12930-12935, 2010.

[8] R. Sierens and E. Rosseel. Variable Composition Hydrogen/Natural Gas Mixtures for Increased Engine Efficiency and Decreased Emissions. *Journal of Engineering for Gas Turbines and Power*, 122(1): 135, 2000.

[9] F. Ma et al. Performance and emission characteristics of a turbocharged spark-ignition hydrogen-enriched compressed natural gas engine under wide-open throttle operating conditions. *International Journal of Hydrogen Energy*, 35(22): 12502-12509, 2010.

[10] A. Yilmaz, E. Uludamar, and K. Aydin. Effect of hydroxy (HHO) gas addition on performance and exhaust emissions in compression ignition engines. *International Journal of Hydrogen Energy*, 35(20): 11366-11372, 2010.

[11] C. Ji and S. Wang. Effect of hydrogen addition on combustion and emissions performance of a spark ignition gasoline engine at lean conditions. *International Journal of Hydrogen Energy*. 34(18): 7823-7834, 2009.

[12] S. Verhelst. Recent progress in the use of hydrogen as a fuel for internal combustion engines. *International Journal of Hydrogen Energy*. 39(2): 1071-1085, 2014.

[13] T. Ismail, K. Ramzy, M. Abelwhab, B. Elnaghi, M. Abd El-Salam, and M. Ismail. Performance of hybrid compression ignition engine using hydroxy (HHO) from dry cell. *Energy Conversion and Management*, 155: 287-300, 2018.

[14] A. Al-Rousan and S. Musmar. Effect of anodes-cathodes inter-distances of HHO fuel cell on gasoline engine performance operating by a blend of HHO. *International Journal of Hydrogen Energy*, 43(41): 19213-19221, 2018.

[15] G. Valencia, A. Fontalvo, Y. Cárdenas, J. Duarte, and C. Isaza. Energy and Exergy Analysis of Different Exhaust Waste Heat Recovery Systems for Natural Gas Engine Based on ORC. *Energies*, 12(12), 2378, 2019.

[16] A. Al-Rousan and S. Musmar. Effect of anodes-cathodes inter-distances of HHO fuel cell on gasoline engine performance operating by a blend of HHO. *International Journal of Hydrogen Energy*, 43(41): 19213-19221, 2018.

[17] B. Subramanian and S. Ismail. Production and use of HHO gas in IC engines. *International Journal of Hydrogen Energy*, 43(14): 7140-7154, 2018.

[18] Y. Petrov, J. Schosger, Z. Stoynov and F. de Bruijn. Hydrogen evolution on nickel electrode in synthetic tap water – alkaline solution. *International Journal of Hydrogen Energy*, 36(20): 12715-12724, 2011.

[19] F. Consuegra, A. Bula, W. Guillín, J. Sánchez, and J. Duarte Forero. Instantaneous in-Cylinder Volume Considering Deformation and Clearance due to Lubricating Film in Reciprocating Internal Combustion Engines. *Energies*, 12(8), 1437, 2019.

